



Science Arts & Métiers (SAM)

is an open access repository that collects the work of Arts et Métiers Institute of Technology researchers and makes it freely available over the web where possible.

This is an author-deposited version published in: <https://sam.ensam.eu>
Handle ID: <http://hdl.handle.net/10985/8823>

To cite this version :

Seifeddine BENELGHALI, Mohamed BENBOUZID, Jean-Frederic CHARPENTIER - Comparison of PMSG and DFIG for Marine Current Turbine Applications - In: Electrical Machines (ICEM), 2010 XIX International Conference on, Italy, 2010-09 - Proceedings of the International Conference on Electrical Machines - 2010

Any correspondence concerning this service should be sent to the repository

Administrator : scienceouverte@ensam.eu



Comparison of PMSG and DFIG for Marine Current Turbine Applications

S. Benelghali, M.E.H. Benbouzid and J.F. Charpentier

Abstract—Emerging technologies for marine current turbine are mainly relevant to works that have been carried out on wind turbines and ship propellers. It is then obvious that many electric generator topologies could be used for marine current turbines. As in the wind turbine context, doubly-fed induction generators and permanent magnet generators seems to be attractive solutions to be used to harness the tidal current energy. In this paper, a comparative study between these two generators type is presented and fully analyzed in terms of generated power, maintenance and operation constraints. This comparison is done for the Raz de Sein site (Brittany, France) using a multiphysics modeling simulation tool. This tool integrates, in a modular environment, the resource model, the turbine hydrodynamic model and the generators models.¹

Index Terms—Marine Current Turbine (MCT), Doubly-Fed Induction Generator (DFIG), Permanent Magnet Synchronous Generator (PMSG), modeling, Maximum Power Point Tracking (MPPT).

NOMENCLATURE

ρ	= Fluid density;
A	= Cross-sectional area of the marine turbine;
V_{tides}	= Fluid speed;
C_p	= Power coefficient;
C	= Tide coefficient;
$V_{st} (V_{nt})$	= Spring (neap) tide current speed;
$s, (r)$	= Stator (rotor) index (superscripts);
d, q	= Synchronous reference frame index;
$V (I)$	= Voltage (Current);
$P (Q)$	= Active (Reactive) power;
ϕ	= Flux;
$T_{em} (T_m)$	= Electromagnetic torque (mechanical torque);
R	= Resistance
$L (M)$	= Inductance (mutual inductance);
σ	= Total leakage coefficient, $\sigma = 1 - M^2/L_s L_r$;
θ_r	= Rotor position;
$\omega_r, (\omega_s)$	= Angular speed (synchronous speed);
sl	= Slip;
f	= Viscosity coefficient;
J	= Rotor Inertia;
p	= Pole pair number;
s	= Derivative operator.

I. INTRODUCTION

Only a fraction of the global ocean energy resource is to be found in sites which are economically feasible to explore with available technology. However, this fraction could still make a considerable contribution to electricity supply. This is the reason why the marine renewable sector is currently the focus

S.E. Ben Elghali and J.F. Charpentier are with the French Naval Academy Research Institute (IRENav EA 3634), French Naval Academy, Lanveoc-Poulmic, CC 600, 29240 Brest Cedex 9, France (e-mail: seiffeddine.ben_elghali@ecole-navale.fr, jean-frederic.charpentier@ecole-navale.fr).

M.E.H. Benbouzid is the University of Brest, EA 4325 LBMS, Rue de Kergoat, CS 93837, 29238 Brest Cedex 03, France (e-mail: Mohamed.Benbouzid@univ-brest.fr).

of much industrial and academic research around the world [1-2]. Sites with attractive wave climate and intense tidal currents are abundant in the vicinity of the European coastline. It has been shown that 48% of the European tidal resource is in the UK, 42% in France, and 8% in Ireland. Three examples in France are shown in Fig. 1. The Raz Blanchard situated in Cap de la Hague, the Raz de Sein and the Fromveur channel in Brittany experiences extreme tidal currents which can exceed 8 knots and leads to a large amount of kinetic energy flux. Considering the main projects for harnessing tidal energy, over the world, it can be noticed that a lot of technological solutions have been proposed and tested in order to found the optimal ones [3]. Therefore, it was necessary to develop simulation environments to estimate the marine current turbines efficiency and quantify the potential of generating electricity from these various sites.

For that purpose, the paper authors have previously elaborated such an environment [4-5]. Indeed, this tool associates model of the resource, hydrodynamic turbine model and electrical generators models in a multiphysics approach. These models were integrated in the Matlab-Simulink[®] environment as Simulink blocks. This method allows a good modularity of the simulator. This MCT simulator is therefore very useful to estimate the relevance a technological solution for a given site.

In this paper, this MCT simulator is used to estimate the harnessed power from a DFIG- and a PMSG-based marine current turbine. To highlight differences between the considered technologies, a variable-speed control approach based on an MPPT strategy is used to carry-out simulations. The two technology choices are then fully analyzed in terms of generated power, maintenance and operating constraints.

II. MARINE CURRENT TURBINE MODELING

The global scheme for a grid-connected marine current turbine is given by Fig. 2. Considering this scheme it can be noticed that a global multiphysics approach must be done to study the behavior of an MCT. So a simulation tool able to predict the behavior of such a system must comprise the resource, the hydrodynamic turbine, the generator, the drive and the grid connection models.

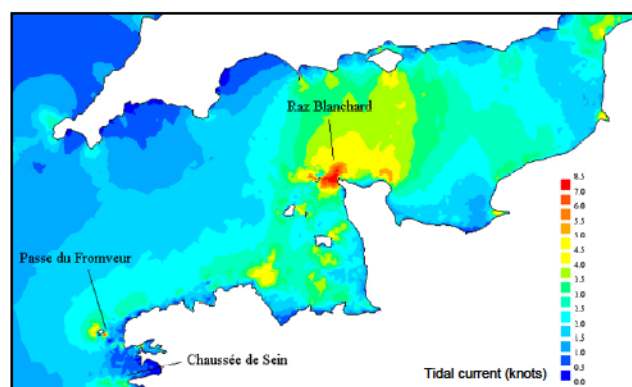


Fig. 1. Raz Blanchard, Fromveur, and Raz de Sein sites in the French western coast.

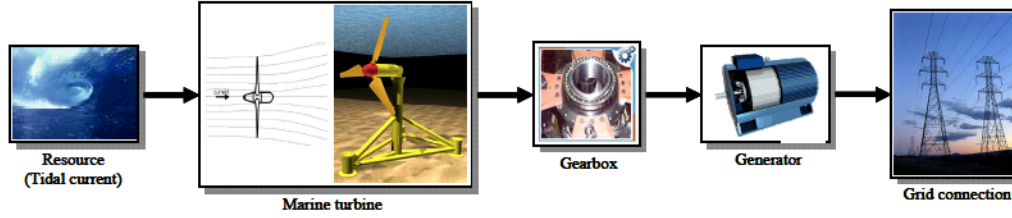


Fig. 2. Marine current turbine global scheme.

A. The Resource Model

1) *Resource potential.* The total kinetic power in a marine current turbine has a similar dependence to that of a wind turbine and is governed by the following equation [6].

$$P = \frac{1}{2} \rho A V_{tides}^3 \quad (1)$$

However, an MCT can only harness a fraction of this power due to losses and (1) is modified as follows.

$$P = \frac{1}{2} \rho C_p A V_{tides}^3 \quad (2)$$

For marine turbines, C_p is estimated to be in the range 0.35–0.5 [8]. Thus, the extracted power depends mainly on the tidal velocities and the turbine sizes (Fig. 3). Therefore, the chosen sites must be characterized by high velocity current coupled with appropriate depth. It also can be noticed that the power output as well as the size of a classical tidal turbine are extremely promising in comparison with wind turbine. Indeed, this due to the sea water huge density and to the current velocity.

2) *Resource model.* The astronomic nature of this resource makes it predictable, to within 98% accuracy for decades, and mainly independent of prevailing weather conditions. This predictability is critical to a successful integration of renewable energy in the electrical grid. Tidal current data are given by the national hydrographic and oceanographic services of major countries. In France, these data are given by the SHOM (French Navy Hydrographic and Oceanographic Service) and are available for various locations in chart form. As an example, the SHOM available charts give, for a specific site, the current velocities for spring and neap tides. These values are given at hourly intervals starting at 6 hours before high waters and ending 6 hours after. Therefore, knowing tides coefficient, it is easy to derive a simple and practical model for tidal current speeds.

$$V_{tides} = V_{nt} + \frac{(C - 45)(V_{st} - V_{nt})}{95 - 45} \quad (3)$$

Where 95 and 45 are respectively the spring and neap tide medium coefficient.

This first-order model is then used to calculate the tidal velocity each hour. The implemented model will allow the user to compute tidal velocities in a predefined time range. Figure 4 shows the model output for a month (March 2007) and for a year (2007). This adopted resource model has several advantages including its modularity and its simplicity. Indeed, the marine turbine site can be changed, the useful current velocity can be adapted, and the time range taken into account can also be adapted from any simulation time. It is also possible to integrate to this resource model swell and turbulence perturbations as shown in [5].

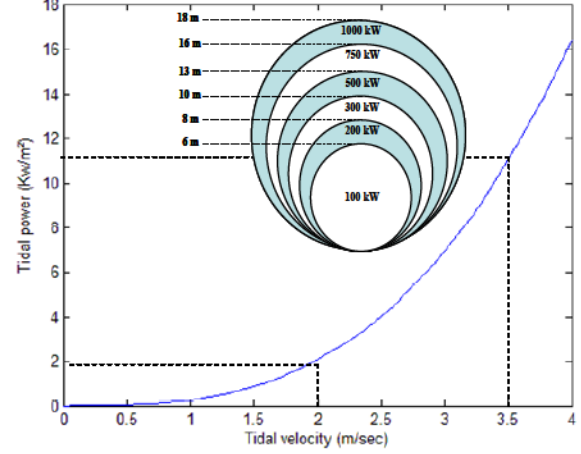


Fig. 3. The harnessed tidal power and power ratings versus the turbine diameter.

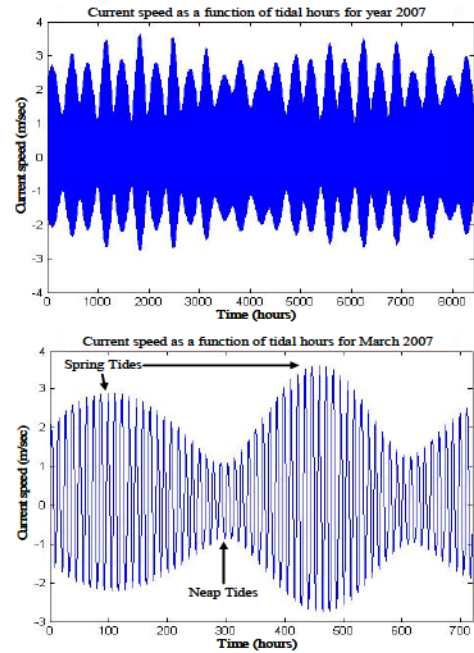


Fig. 4. Tidal velocity in the Raz de Sein for the year 2007 and March 2007.

B. The Turbine Rotor Model

The harnessing of the energy in a tidal flow requires the conversion of kinetic energy in a moving fluid, in this case water, into the motion of a mechanical system, which can then drive a generator. It is not too surprising, therefore, that many developers suggest using technology that mirrors that which has been successfully utilized to harness the wind, which is also a moving fluid [3]. Moreover, much of the technology is based upon the use of horizontal axis turbines. Therefore, much can be transferred from the modeling and operation of wind turbines. There are, however, a number of fundamental differences in the design and operation of marine turbines. Particular differences entail changes in force loadings, immersion depth, different stall characteristics, and the possible occurrence of cavitations [7].

Wind or marine turbine rotor performance calculation refers to the interaction of the turbine rotor with the incoming fluid. For wind turbine design, the treatment of rotor performance in many current design codes is based on Glauert well-known, and well established Blade Element Momentum (BEM) theory. The BEM method can therefore be used for the marine turbine rotor modeling [8]. For illustration, Fig. 5 shows some performance results obtained with this method for a 1.44 m diameter three-blade rotor. This method has been validated with experimental results. It is relatively simple and computationally fast meeting the requirements of accuracy and control loop computational speed.

C. The Generator Model

Much of the technology that has been suggested for tidal current energy extraction is reminiscent of that used for wind applications. It is then obvious that some wind electric generator topologies could be used for marine turbines [9]. Table 1 briefly summarizes the pros and cons of the major generator topologies. In this table, many topologies seem a priori to be exploitable for tidal turbines.

In this paper we have chosen to focus on two of these generator technologies. The first one is the Doubly-Fed Induction Generator which is extensively used for wind turbines. The second one is the Permanent Magnet Synchronous Generator. It has been chosen because this technology is characterized by a low maintenance level, high compactness and allows using nonconventional solutions for the turbine generator integration [10-11].

1) *DFIG model.* The DFIG-based MCT, as for wind turbines, will offer several advantages including variable speed operation, and four-quadrant active and reactive power capabilities [12]. Such system also results in lower converter costs and lower power electronics losses compared to a system based on a fully fed synchronous generator with full-rated converter.

The control system is usually defined in the synchronous $d-q$ frame fixed to either the stator voltage or the stator flux [12]. The generator dynamic model written in a synchronously rotating frame $d-q$ is given by (4). A schematic diagram of a DFIG-based generation system is shown in Fig. 6.

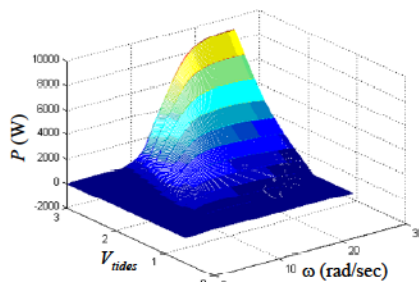
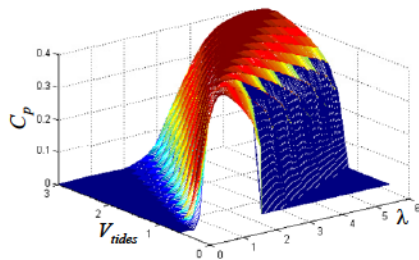


Fig. 5. Calculated hydrodynamics performance of a 1.44 m diameter turbine.

TABLE 1.
GENERATOR TOPOLOGIES COMPARISON

Type	Pros	Cons
Induction Generator	<ul style="list-style-type: none"> ✓ Full speed range ✓ No brushes on the generator ✓ Complete control of reactive and active power ✓ Proven technology 	<ul style="list-style-type: none"> * Full scale power converter * Need for gear
Synchronous Generator	<ul style="list-style-type: none"> ✓ Full speed range ✓ Possible to avoid gear ✓ Complete control of reactive and active power 	<ul style="list-style-type: none"> * Small converter for field * Full scale power converter * Multipole generator (big and heavy) in case of direct driven topology
Permanent Magnet Synchronous Generator	<ul style="list-style-type: none"> ✓ Full speed range ✓ Possible to avoid gear ✓ Complete control of reactive and active power ✓ Brushless (low maintenance) ✓ No power converter for field 	<ul style="list-style-type: none"> * Full scale power converter * Multipole generator (big and heavy) * Permanent magnets needed
Doubly-Fed Induction Generator	<ul style="list-style-type: none"> ✓ Limited speed range -30% to 30% around synchronous speed ✓ Inexpensive small capacity PWM Inverter ✓ Complete control of reactive and active power 	<ul style="list-style-type: none"> * Need slip rings * Need for gear

$$\begin{cases}
 \frac{d\phi_{ds}}{dt} = V_{ds} + R_s I_{ds} + \omega_s \phi_{qs} \\
 \frac{d\phi_{qs}}{dt} = V_{qs} + R_s I_{qs} - \omega_s \phi_{ds} \\
 \frac{d\phi_{dr}}{dt} = V_{dr} + R_r I_{dr} + \omega_r \phi_{qr} \\
 \frac{d\phi_{qr}}{dt} = V_{qr} + R_r I_{qr} - \omega_r \phi_{dr} \\
 \phi_{ds} = -L_s I_{ds} - M I_{dr} \\
 \phi_{qs} = -L_s I_{qs} - M I_{qr} \\
 \phi_{dr} = -L_r I_{dr} - M I_{ds} \\
 \phi_{qr} = -L_r I_{qr} - M I_{qs} \\
 T_{em} = pM(I_{qs} I_{dr} - I_{ds} I_{qr}) \\
 J \frac{d\omega}{dt} = T_{em} - T_m - f\omega
 \end{cases} \quad (4)$$

2) *PMSG model.* The PMSG choice allows direct-drive systems that avoid gearbox use. This solution is very advantageous as it leads to low maintenance constraints. However, in such design, the generator is completely decoupled from the grid by a voltage source full power converter (AC/DC/AC) connected to the stator (Fig. 7).

The PMSG dynamic equations are expressed in the $d-q$ reference frame. The model of electrical dynamics in terms of voltage and current can be given as (5) [13].

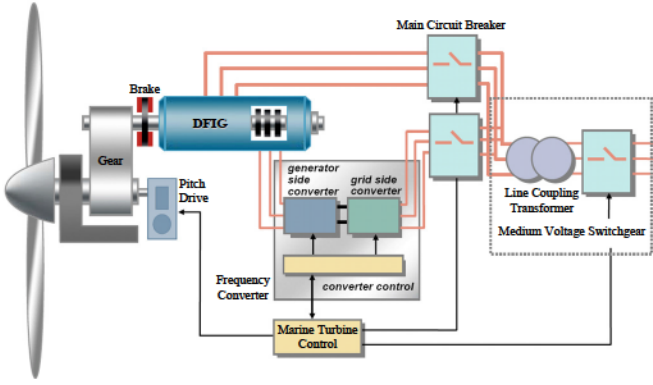


Fig. 6. Schematic diagram of a DFIG-based generation system.

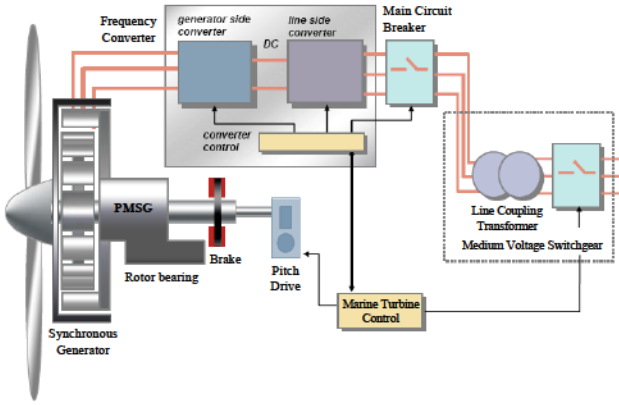


Fig. 7. Schematic diagram of a PMSG-based generation system.

$$\begin{cases} V_d = RI_d + L_d \frac{dI_d}{dt} - \omega L_q I_q \\ V_q = RI_q + L_q \frac{dI_q}{dt} + \omega L_d I_d - \omega \phi_f \end{cases} \quad (5)$$

The electromagnetic torque in the rotor is written as

$$T_{em} = \frac{3}{2} p [(L_d - L_q) I_d I_q - \phi_f I_q] \quad (6)$$

IV. VARIABLE SPEED CONTROL

In order to illustrate the variable speed control, a low-power variable-speed fixed-pitch MCT driven DFIG and PMSG has been simulated. The proposed variable speed control strategy is based on an MPPT. First, the optimal speed reference ω_{ref} at each time is computed from the knowledge of the current velocity. This speed reference corresponds to the maximum power which can be mechanically extracted by the turbine for the fluid velocity value. Then, a classical speed control of the generator ensures the convergence of the rotor speed to ω_{ref} based on PI control. The above proposed control strategy for a DFIG-based MCT is illustrated by Fig. 8.

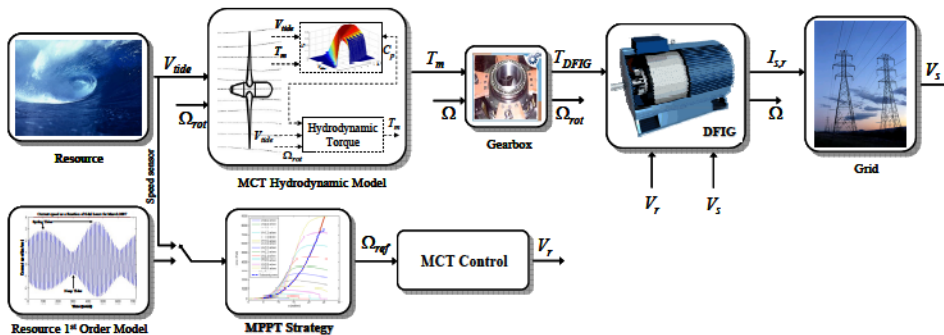


Fig. 8. Variable speed control for a DFIG-based MCT.

For speed references given by the MPPT strategy, the DFIG-based MCT control performances are shown in Figs. 9 and 10 respectively illustrating the rotor speed tracking performance and the generated active power. The simulation time has been reduced to seconds to limit the computation time to realistic ones. In real-world application, the system mechanical dynamics will be slower than in simulations. The variable speed control strategy is tested by using a resource first-order model for a marine current turbine of 1.44 m diameter and 7.5-kW DFIG. This low power corresponds to typical lab size test bench used for experimental validation.

The main merit of the DFIG is its capability to deliver constant voltage and frequency output for $\pm 30\%$ speed variation around conventional synchronous speed. It can be noticed that another choice for the speed variation range is possible (between 30 and 50% are the more often used). This 30% variation speed choice is directly related to a low power sizing of the rotor converter.

The same variable speed strategy has been adopted for PMSG-based MCT control. The obtained results show good tracking performances of the PMSG rotor speed (Fig. 11). Figure 12 illustrates the generated active power. Even if in real world and for high power turbines a direct driven PMSG must be used for this application, it can be noticed that in our case the simulations are presented for a PMSG with a gearbox. Indeed the first goal of these simulations was experimental validation. These simulation results were validated in a test bench including a gearbox where the PMSG was driven by a DC motor which emulates the hydrodynamic loads [14].

In the two cases there are minor differences between the predicted and simulated power. These differences are mainly due to the type of control which is based on speed control and not on a direct power control.

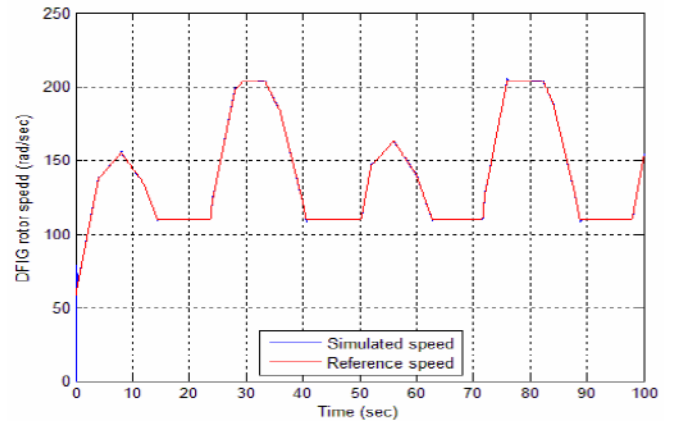


Fig. 9. The DFIG rotor speed and its reference.

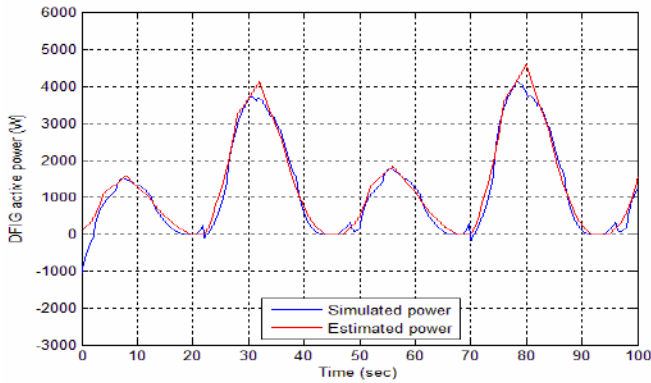


Fig. 10. The DFIG active power.

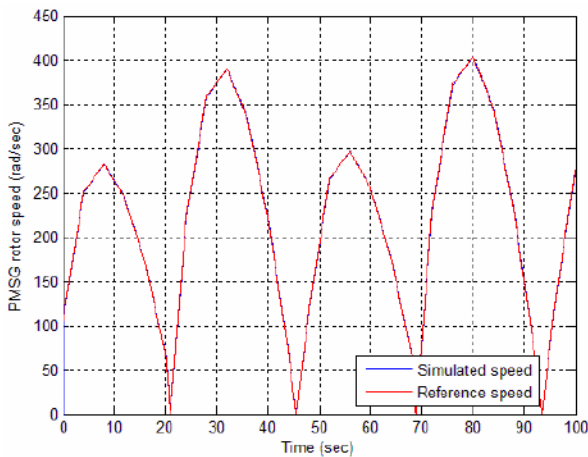


Fig. 11. The PMSG rotor speed and its reference.

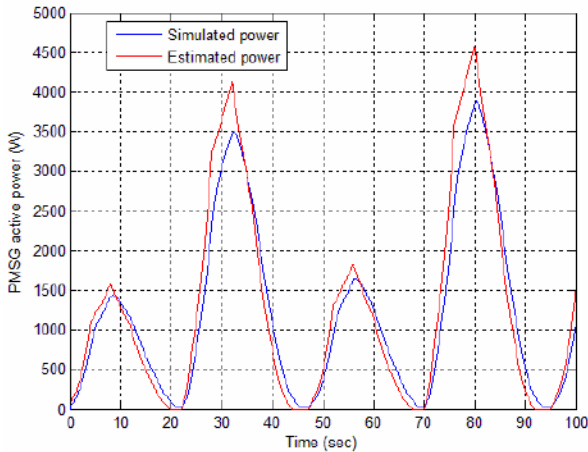


Fig. 12. The PMSG active power.

V. COMPARATIVE STUDY

The comparison of different generator systems in the literature is generally discussed with criteria based on the energy yield and cost.

The DFIG appears slightly more advantageous than the PMSG since it is a lightweight and low cost concept [15]. Indeed, the converter for DFIG-based MCT is dimensioned only for the 25% of the rated power, which justify the success of these systems for wind applications. But the particular context of marine applications imposes different constraints. The marine current turbine will be installed in sites with strong currents and difficult to access. Therefore, minimizing

maintenance is a fundamental aspect. A direct-drive PMSG requires less maintenance than DFIG which needs a regular maintenance, in particular for the gearbox and the slip rings.

For the first criteria, we have calculated the annual produced power for the two technologies based on tidal current data from the Raz de Sein (Brittany, France), a 10-m diameter 100-kW turbine. This power ratings correspond to the major prototypes that have been recently tested [3]. Figure 13 shows the Raz de Sein site tidal histogram and Figs. 14 and 15 illustrate the annual power extracted by each technology for this rated power MCT. In this case and for calculation time reasons, simulations are only based on the use of the resource and the turbine hydrodynamic model. This means that the turbine generator speed control is considered to be able to perfectly track the MPPT reference speed. This assumption appears to be realistic considering simulations in low power cases previously presented in Fig. 9 and 10.

The harnessed power from DFIG-based MCT is estimated about 1530 MWh/year. However the PMSG-based MCT can extract up to 1916 MWh/year. Thus, over a year, there is a difference about 25% between the two technologies and this percentage will grow up when using a greater turbine. This difference is due to speed restrictions imposed to the DFIG. Indeed, the speed references are limited to $\pm 30\%$ of the rated speed. These limited speeds, when imposed as reference, correspond generally to a poor C_p leading to a reduced extracted power.

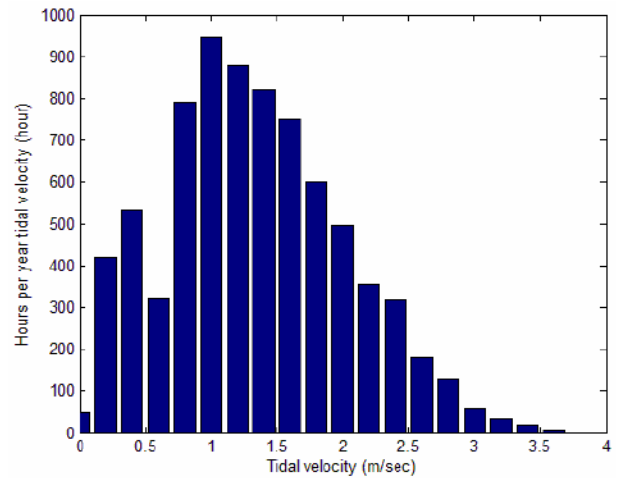


Fig. 13. Raz de Sein site tidal histogram.

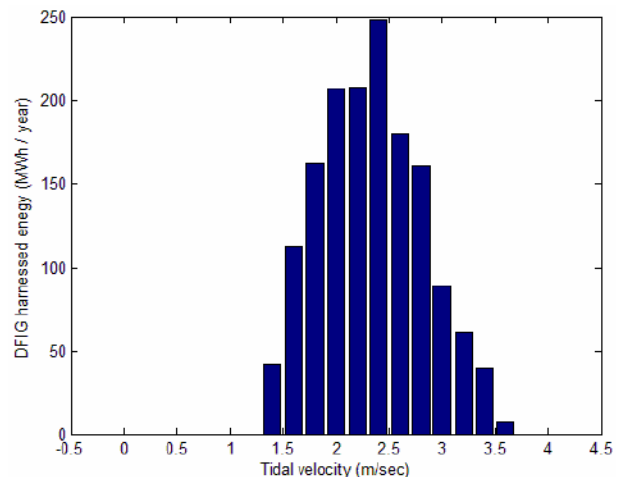


Fig. 14. DFIG-based MCT harnessed energy histogram in one year.

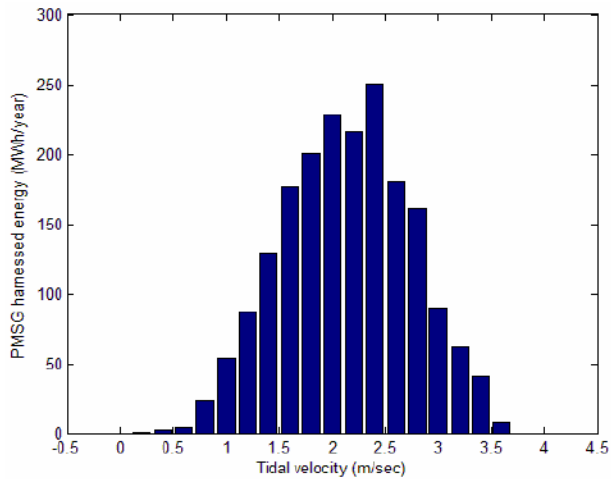


Fig. 15. PMSG-based MCT harnessed energy histogram in one year.

VI. CONCLUSION

According to the comparative study, the permanent magnet synchronous generator-based MCT has the highest energy yield. It can be concluded that, if solutions based on a doubly fed induction generator have been very successful for wind turbine applications, it is probably not the case in marine turbine applications except in special cases. Moreover, PMSG direct-drives seem much more interesting for marine applications which requires very robust and maintenance free systems.

REFERENCES

- [1] C.M. Johnstone, K. Nielsen, T. Lewis, A. Sarmento and G. Lemonis, "EC FPVI co-ordinated action on ocean energy: A European platform for sharing technical information and research outcomes in wave and tidal energy systems," *Renewable Energy*, vol. 31, pp. 191-196, 2006.
- [2] 2005 IEEE Power Engineering Society General Meeting Panel Session, "Harnessing the untapped energy potential of the oceans: Tidal, wave, currents and OTEC," San Francisco (USA), June 2005.
- [3] S. Benelghali, M.E.H. Benbouzid and J.F. Charpentier, "Marine tidal current electric power generation technology: State of the art and current status," in *Proceedings of IEEE IEMDC'07, Antalya (Turkey)*, vol. 2, pp. 1407-1412, May 2007.
- [4] S. Benelghali, M.E.H. Benbouzid and J.F. Charpentier, "Modeling and control of a marine current turbine driven doubly-fed induction generator," *IET Renewable Power Generation*, vol. 4, n°1, pp. 1-11, January 2010.
- [5] S. Benelghali, R. Balme, K. Le Saux, M.E.H. Benbouzid, J.F. Charpentier and F. Hauville, "A simulation model for the evaluation of the electrical power potential harnessed by a marine current turbine," *IEEE Journal on Oceanic Engineering*, vol. 32, n°4, pp. 786-797, October 2007.
- [6] J.S. Couch and I. Bryden, "Tidal current energy extraction: Hydrodynamic resource characteristics," *Proc. IMechE, Part M: Journal of Engineering for the Maritime Environment*, vol. 220, n°4, pp. 185-194, 2006.
- [7] W.M.J. Batten, A.S. Bahaj, A.F. Molland and J.R. Chaplin, "Hydrodynamics of marine current turbines," *Renewable Energy*, vol. 31, pp. 249-256, 2006.
- [8] G. Mattarolo, P. Caselitz and M. Geyler, "Modelling and simulation techniques applied to marine current turbine," in *Proceedings of the 2006 International Conference on Ocean Energy*, Bremerhaven (Germany), 2006.
- [9] J.W. Park, K.W. Lee and H.J. Lee, "Wide speed operation of a doubly-fed induction generator for tidal current energy," in *Proceedings of the IEEE IECON'2004, Busan (South Korea)*, vol. 2, pp. 1333-1338, 2004.
- [10] M. Chinchilla, S. Arnaltes and J.C. Burgos, "Control of permanent-magnet generators applied to variable-speed wind-energy systems connected to the grid," *IEEE Trans. Energy Conversion*, vol. 21, n°1, pp. 130-135, March 2006.
- [11] L. Drouen, J.F. Charpentier, E. Semail and S. Clenet, "Study of an innovative electrical machine fitted to marine current turbine," in *Proceedings of the IEEE OCEAN'07, Aberdeen (Scotland)*, 6 pp., June 2007.
- [12] S. Müller, M. Deicke and R.W. De Doncker, "Doubly fed induction generator systems," *IEEE Industry Applications Magazine*, vol. 8, n°3, pp. 26-33, May-June 2002.
- [13] K. Tan and S. Islam, "Optimum control strategies in energy conversion of PMSG wind turbine system without mechanical sensors," *IEEE Trans. Energy Conversion*, vol. 19, n°2, pp. 392-399, June 2004.
- [14] S. Benelghali, M.E.H. Benbouzid, J.F. Charpentier, T. Ahmed-Ali and I. Munteanu, "Experimental validation of a marine current turbine simulator: Application to a PMSG-based system second-order sliding mode control," *IEEE Trans. Industrial Electronics*, 10.1109/TIE.2010.2050293, 2010.
- [15] D. Bang, H. Polinder, G. Shrestha and J.A. Ferreira, "Review of generator systems for direct-drive wind turbines," in *Proceedings of the EWEC'08, Brussels (Belgium)*, March-April 2008.